Article

Identification of Nine lncRNAs Signature for Predicting Survival Benefit of Melanoma Patients Treated with Immune Checkpoint Inhibitors

Jian-Guo Zhou1,[2,3*], Bo Liang[4*], Jian-Guo Liu[5*], Su-Han Jin[5], Si-Si He[1], Benjamin Frey[2,3], Ning Gu[4], Rainer Fietkau[2,3], Markus Hecht[2,3], Hu Ma[1#]and Udo S. Gaipl[2,3#]

1 Department of Oncology, The second affiliated Hospital of Zunyi Medical University, Zunyi, China
2 Department of Radiation Oncology, Universitätsklinikum Erlangen, Erlangen, Germany
3 Comprehensive Cancer Center Erlangen-EMN, Erlangen, Germany
4 Affiliated Nanjing Hospital of Chinese Medicine, Nanjing University of Chinese Medicine, Nanjing, China
5 Special Key Laboratory of Oral Diseases Research, Stomatological Hospital Affiliated to Zunyi Medical University, Zunyi, China

* JGZ, BL, JGL contributed equally as first authors

# HM and USG contributed equally as senior authors

Correspondence:

Prof. Dr. Udo Gaipl

Head of Radiation Immunobiology

Department of Radiation Oncology

Universitätsklinikum Erlangen

Friedrich-Alexander-Universität Erlangen-Nürnberg (FAU)

Universitätsstraße 27, 91054 Erlangen, Germany

Tel Office: +49 (0)9131-85-44258

Fax: +49 (0)9131-85-39335

E-mail address: udo.gaipl@uk-erlangen.de

Prof. Dr. Hu Ma

Director of Department of Oncology

Vice President of the second affiliated Hospital of Zunyi Medical University

Intersection of Xinlong And Xinpu Avenue, 563000, Zunyi, China
E-mail address: mahuab@163.com

Abstract: Immune checkpoint inhibitors (ICI) have been widely used in melanoma, but to identify melanoma patients with survival benefit from ICI is still a big challenge. There is an urgent need for prognostic signatures improving the prediction of immunotherapy responses of cancer patients. We used data from EMBL-EBI database and analyzed RNA-seq information and clinical profiles in melanoma. Weighted gene co-expression network analysis (WGCNA) was used to identify the key module, then nonnegative matrix factorization (NMF) was conducted to cluster patients into two different cluster and compared them regarding overall survival (OS) and progression-free survival (PFS). Subsequently, the differentially expressed genes (DEGs) between different clusters were identified, and their function and pathway annotation were performed. 91 melanoma biopsies with complete survival information were included in our analyses and we first identified the key module (magenta) by WGCNA, then identified nine prognostic lncRNAs (ENSG00000258869, ENSG00000179840, ENSG00000206344, ENSG00000226777, ENSG00000205018, ENSG00000204261, ENSG00000163597, ENSG00000197536, and ENSG00000263069) signature that predicted for OS and PFS in patients treated with ICI by NMF. Finally, enrichment analysis showed that the functions of DEGs between two consensus clusters were mainly related to the immune process and treatment. In summary, the nine lncRNAs signature is a novel effective predictor for OS and PFS in melanoma patients treated with ICI.

Keywords: lncRNA; melanoma; prognosis; immune checkpoint inhibit; WGCNA; NMF

1. Introduction

Melanoma is one of the most aggressive malignant skin tumors, and the incidence has been increasing worldwide in recent decades [1,2]. Since the US Food and Drug Administration (FDA) and European Medicines Agency (EMA) approved a variety of immune checkpoint inhibitors (ICI) therapies for advanced melanoma in 2011, the overall mortality of advanced melanoma fell by 17.9% from 2013 to 2016 [3], but it is still at a very high level [4].

During the last years, biomarkers for effectiveness of tumor immunotherapy, including genomic instability as described by microsatellite instable (MSI) or tumor mutational burden (TMB) status, and immune cell infiltration into tumors, have been defined [5]. As one of the cancer types with high TMB and high immune cell infiltration, melanoma can be considered for immunotherapy [5]. Despite all efforts of early diagnosis, metastatic melanoma still has a poor prognosis and remains a challenge for treating physicians. Existing ICI therapies include the blockade of programmed death 1 (PD-1)/programmed death-ligand 1 (PD-L1) and cytotoxic T-lymphocyte antigen 4 (CTLA-4) pathway. Ipilimumab (an anti-CTLA-4 monoclonal antibody) [6], nivolumab (an anti-PD-1 agent) [7], and pembrolizumab (an anti-PD-1 monoclonal antibody) [8] monotherapy all improve relapse/recurrence-free survival of stage III melanoma patients. Moreover, anti-PD-1 monoclonal antibodies indicate superior overall/recurrence-free survival versus anti-CTLA-4 agent for advanced melanoma [7,9,10]. Combination therapy with nivolumab plus ipilimumab led to improved outcomes compared with ipilimumab alone [11-14]. The results from the CheckMate 067 and 069 trials indicate longer treatment-free survival in nivolumab plus ipilimumab (11.1 months) treated patients compared with nivolumab (4.6 months) or ipilimumab (8.7 months) single treatments [15]. Nivolumab combined with ipilimumab had clinically meaningful consistent efficacy [16]. Although the results suggest encouraging survival outcomes with ICI in this population of patients, subgroup analysis demonstrated that both treatments (the nivolumab-plus-ipilimumab combination and nivolumab monotherapy, all ~50%) led to better objective response rates than ipilimumab (~20%), regardless of PD-L1 expression [11-13]. Future research should focus on identifying additional biomarkers to select patients who are most likely to benefit from certain immunotherapies.

Numerous long noncoding RNAs (lncRNAs) have been identified in human genomes [17] and they are nowadays considered as prognosis signatures in various tumors [18,19]. However, there has been limited systematic characterization of these elements in melanoma, especially in melanoma patients treated with ICI. Here, we identified nine lncRNAs signature in advanced melanoma

regardless of gender, age, prescriptions, MSI, TMB, and immune cell infiltration by weighted gene co-expression network analysis (WGCNA) and nonnegative matrix factorization (NMF) to determine and predict the prognosis of melanoma patients receiving ICI and their response to ICI.

2. Materials and Methods

2.1. Data source and processing

The transcriptomic profiling (PRJEB23709) [20] were obtained from the European Molecular Biology Laboratory-European Bioinformatics Institute (EMBL-EBI) database [21] (https://www.ebi.ac.uk/ena/data/view/PRJEB23709). Raw RNA-seq reads were aligned to the reference genome (UCSC hg38 with annotations from GRCh38.p13) using STAR [22] (v.2.5.3a). Gene expression was subsequently quantified using RSEM [23] (v.1.3.1). lncRNA annotations were done by gencode.v33.annotation(https://www.gencodegenes.org/human/). Only the inlier samples that were identified by hierarchical cluster analysis via the *hclust* function in WGCNA were included.

2.2. Module construction

Unsigned co-expression modules were constructed using the WGCNA algorithms in R as described previously [24]. We used one-step network construction method to identify co-expression modules through the *blockwiseModules* function in the *WGCNA* package [25]. Before co-expression network construction, the *flashClust* tool in R was utilized to perform hierarchical clustering analysis of the samples with the appropriate threshold value to detect and eliminate the outliers. According to scale-free topology criterion, a soft-thresholding power β (the power values ranged from 1 to 20), which was calculated by the *pickSoftThreshold* function of the WGCNA, was chosen to build an adjacency matrix [25]. In our study, the power of 6 was used for this network.

Then, the topological overlap matrix was constructed based on the adjacency matrix. A dissimilarity matrix was used to detect gene modules (gene sets with high topological overlap) through a dynamic tree cutting algorithm [26,27]. To obtain moderately sized modules, the minimum number of genes was set at 30 and a cutline was chosen to merge modules with similar expression patterns. To identify the relationships between modules and clinical traits, we calculated the correlation between module eigengenes and clinical trait and searched for the most significant associations. The module eigengenes was calculated by the first principal component, which were considered as a representative of the expression patterns of module genes [28]. For each module, we defined the module membership as the correlation of gene expression profile with module eigengene and the gene significance as the absolute value of the correlation between gene and clinical traits. In this study, genes with high module membership in a module were assigned to the module and the module with high gene significance and P value < 0.05 was considered to be highly related to clinical traits. Moreover, we used network-based statistics, which generated a composite statistic value ($Z_{summary}$) using a permutation test to measure the strength of lncRNAs module and expression module preservation, to assess whether the density and connectivity patterns of lncRNAs were also preserved [29]. $Z_{summary} > 10$ implies strong evidence for module preservation[29]. Since the $Z_{summary}$ statistic bias towards a module with a large size[29], a rank-based statistic medianRank, calculated from observed preservation values and conducted no permutation test against background gene modules, was used to measure the relative preservation irrespective of module size [30].

2.3. Identifcation of lncRNAs signature

Although which module was most relevant to clinical features can be identified after WGCNA, we used *survival* package to carry out prognostic survival analysis, including overall survival (OS) and progression-free survival (PFS), as described previously [31]. In addition, the prognostic lncRNAs were intersected with the lncRNAs in different previously established modules to further determine the prognosis related modules and lnRNAs. Only lncRNAs related to OS and PFS, which were named prognostic lncRNAs in the prognostic module, were regarded as lncRNAs signature.

2.4. Consensus clusters

After the identification of prognostic module, we further clustered melanoma population into different consensus clusters though NMF [32] according to the lncRNAs signature, which come from the prognostic lncRNAs. Deposition was repeatedly performed, and its result was aggregated to acquire consensus clustering. The most suitable number of subtypes was decided according to cophenetic coefficient. Ultimately, the lncRNAs signature can distinguish different consensus clusters, and the *survival* package was again applied to perform Kaplan-Meier analysis with the log-rank test to analyze the OS and PFS.

2.5. Subgroup analysis

Considering that two tumor biopsies were collected from one patient in the source data [20], we eliminated all the duplicate patients and then verified the lncRNAs signature again. Moreover, subgroup analysis was also performed for anti-PD-L1 alone or in combination with anti-CTLA-4.

2.6. Functional analysis

Subsequently, the DEGs between different consensus clusters distinguished by the lncRNAs signature were identified by *edgeR* package [33] with the cutoff of fold change >= 2 and $P < 0.05$. Functional analysis were performed using the *clusterProfiler* package [34] to greatly expand our understanding of those lncRNAs signature related functions and their coordinated regulatory networks.

3. Results

3.1. Patient characteristics

PRJEB23709 included 120 patients (158 tumor biopsies) [20] from melanoma patients treated with anti-PD-1 monotherapy (nivolumab or pembrolizumab) or combined anti-PD-1 and anti-CTLA-4 (nivolumab or pembrolizumab combined with ipilimumab). In our study, we included 75 patients (91 tumor biopsies) where data about OS and PFS were available. 41 (50 tumor biopsies) were melanoma patients treated with anti-PD-1 monotherapy and 34 (41 tumor biopsies) were melanoma patients treated with combined anti-PD-1 and anti-CTLA-4, respectively. The patient characteristics are listed in Table 1. A total of 73 tumor biopsies were collected at pre-treatment (PRE) and 18 tumor biopsies were collected at early time points during treatment (EDT), and 16 out of 75 patients had biopsies both at PRE and at EDT. Responders were defined as patients with a Response Evaluation Criteria in Solid Tumors (RECIST) response of complete response (CR), partial response (PR), or stable disease (SD) of greater than 6 months with no progression, and non-responders as progressive disease (PD) or SD for less than or equal to 6 months before disease progression. Among them, 14 patients completely responded, 26 patients partially responded, and 11 patients had SD and 24 patients showed PD, respectively.

Table 1. Patient characteristics.

Features	Monotherapy (N = 41)	Combined Therapy (N = 34)
Gender		
Male	26 (63%)	23 (68%)
Female	15 (37%)	11 (32%)
Age		
> = 60	26 (63%)	13 (38%)
< 60	15 (37%)	21 (62%)
RECIST Response		
CR	4 (10%)	10 (29%)
PR	15 (37%)	11 (32%)
SD	6 (15%)	5 (15%)
PD	16 (39%)	8 (24%)
Survival time		
PFS (days)	271 (80 ~ 891)	508 (89 ~ 635)
OS (days)	607 (169 ~ 1085)	616 (434 ~ 682)
Progressed		
Yes	29 (71%)	15 (44%)
No	12 (29%)	19 (56%)
Status		
Alive	17 (41%)	28 (82%)
Dead	24 (59%)	6 (18%)

Note: Monotherapy: anti-PD-1 monotherapy (nivolumab or pembrolizumab), Combined Therapy: combined anti-PD-1 and anti-CTLA-4 (nivolumab or pembrolizumab combined with ipilimumab), RECIST: Response Evaluation Criteria in Solid Tumors, CR: complete response, PR: partial response, SD: stable disease, PD: progressive disease, PFS: progression-free survival, OS: overall survival.

3.2. WGCNA and key module identification

We obtained data of 16880 lncRNAs from 91 tumor biopsies by transcriptome analysis and the top 4220 most variant lncRNAs were included to construct co-expression networks by WGCNA. To exclude the outliers, we chose 15000 for the cut tree height for the samples (Figure 1A), and 88 samples were included for subsequent analysis. Then we identified the soft-thresholding power β of 6 to construct a scale-free network (Figure 1B&C). As a result, 14 co-expression modules were identified. By gathering similarly expressed lncRNAs, 14 modules were classified to tan, red, turquoise, cyan, purple, brown, yellow, magenta, salmon, pink, blue, green, and black (Figure 2A). Interactions between 14 modules were subsequently analyzed. The heatmap (Figure 2B) demonstrated the topological overlap matrix among all of 4220 lncRNAs in our study, indicating that each module showed independent validation to each other. Then, the correlations between module eigengene, and clinical traits were discovered (Figure 2C). Moreover, we plotted the preservation median rank and $Z_{summary}$ for the modules as a function of module size. Nine modules (tan, turquoise, brown, greenyellow, yellow, magenta, pink, green, and black) showed strong evidence of preservation ($Z_{summary} > 10$) (Figure S1). The module eigengenes in the magenta module showed a higher correlation with PFS, progress, survival status, and RECIST response ($R_{PFS}^2 = 0.38$, $P < 0.0001$;

$R_{progress}^2 = -0.25$, $P = 0.02$; $R_{survival\ status}^2 = -0.21$, $P = 0.05$; $R_{RECIST\ response}^2 = 0.37$, $P < 0.0001$; respectively) (Figure 2C). We therefore chose the magenta module for further analyses.

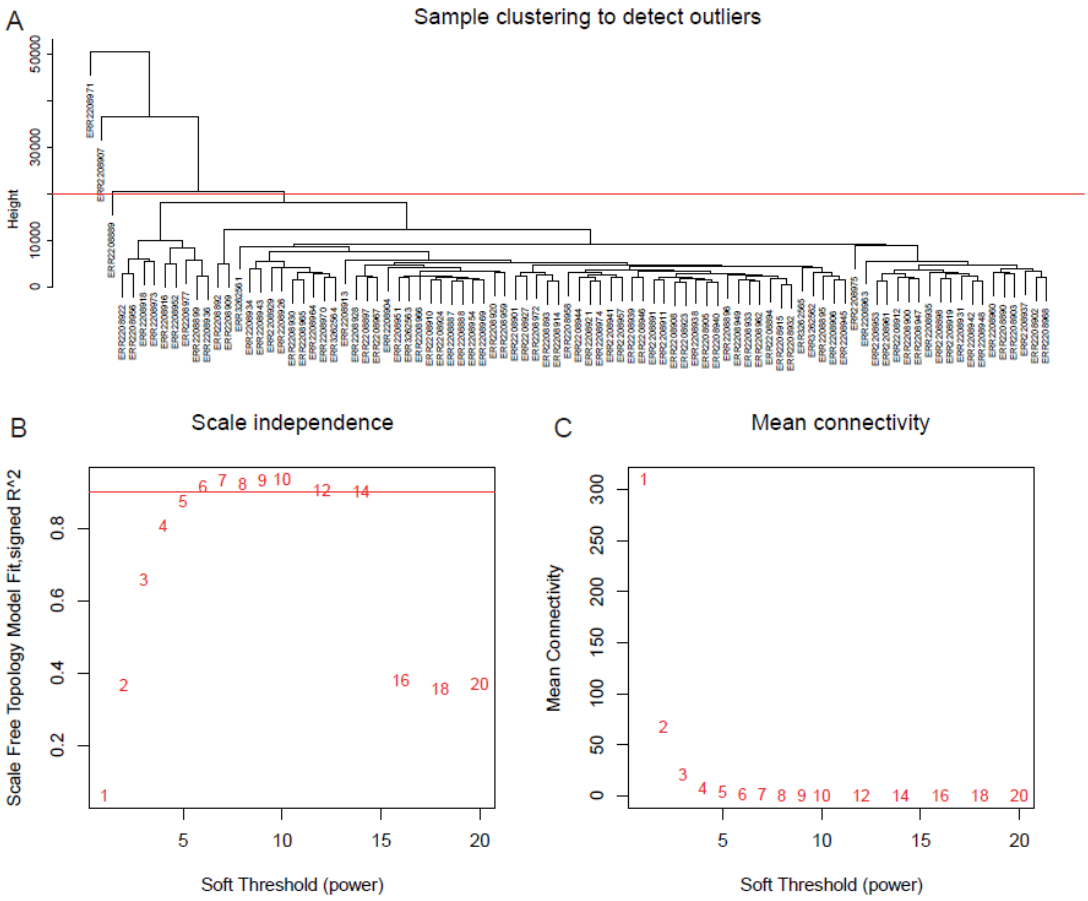

Figure 1. Sample clustering dendrogram and determination of soft-thresholding power in WGCNA. A. Sample clustering dendrogram to detect outliers. B. Analysis of the scale-free fit index for various soft-thresholding power. C. Analysis of the mean connectivity for various soft-thresholding powers.

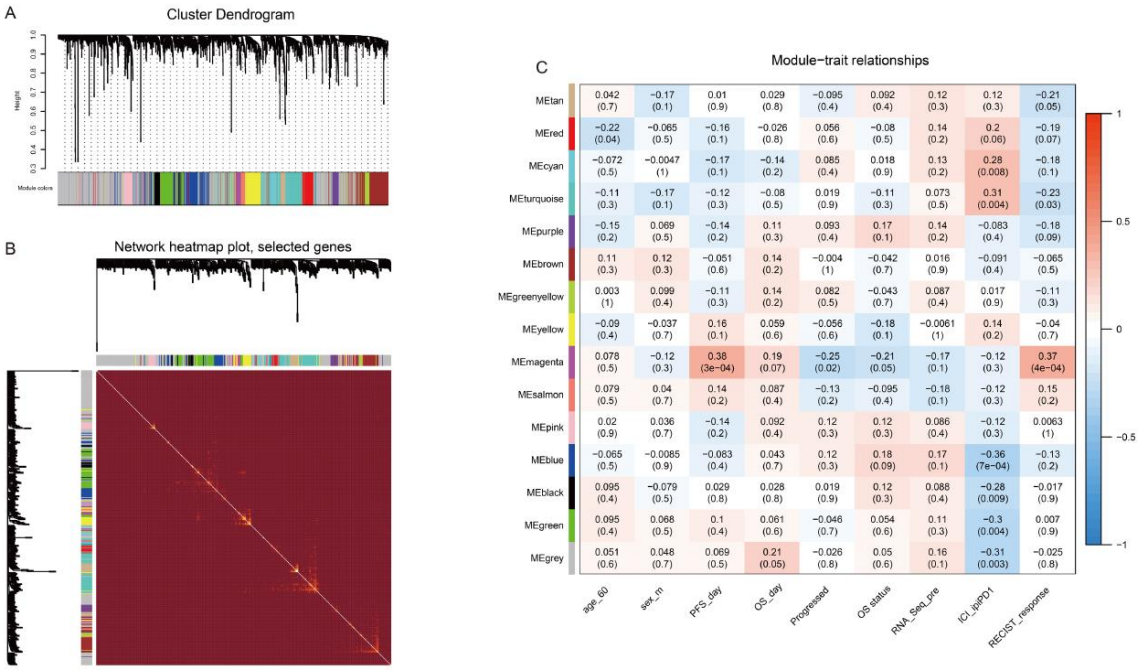

Figure 2. Identification of key module related to OS and PFS by WGCNA. A. Clustering dendrogram of lncRNAs with dissimilarity based on topological overlap together and assigned module colors. B. The heatmap plot of visualizing all modules. C. The module- trait heatmap plot.

3.3. Identification of lncRNAs signature

We found that 174 and 244 lncRNAs were related to OS and PFS, respectively (Table S1). Compared with the lncRNAs in the magenta module, 29 and 38 lncRNAs coincided with those related to OS and PFS, respectively (Figure 3). Interestingly, in this module, 25 lncRNAs related to OS (86.21%) were all related to PFS and thus were regarded as lncRNAs signature.

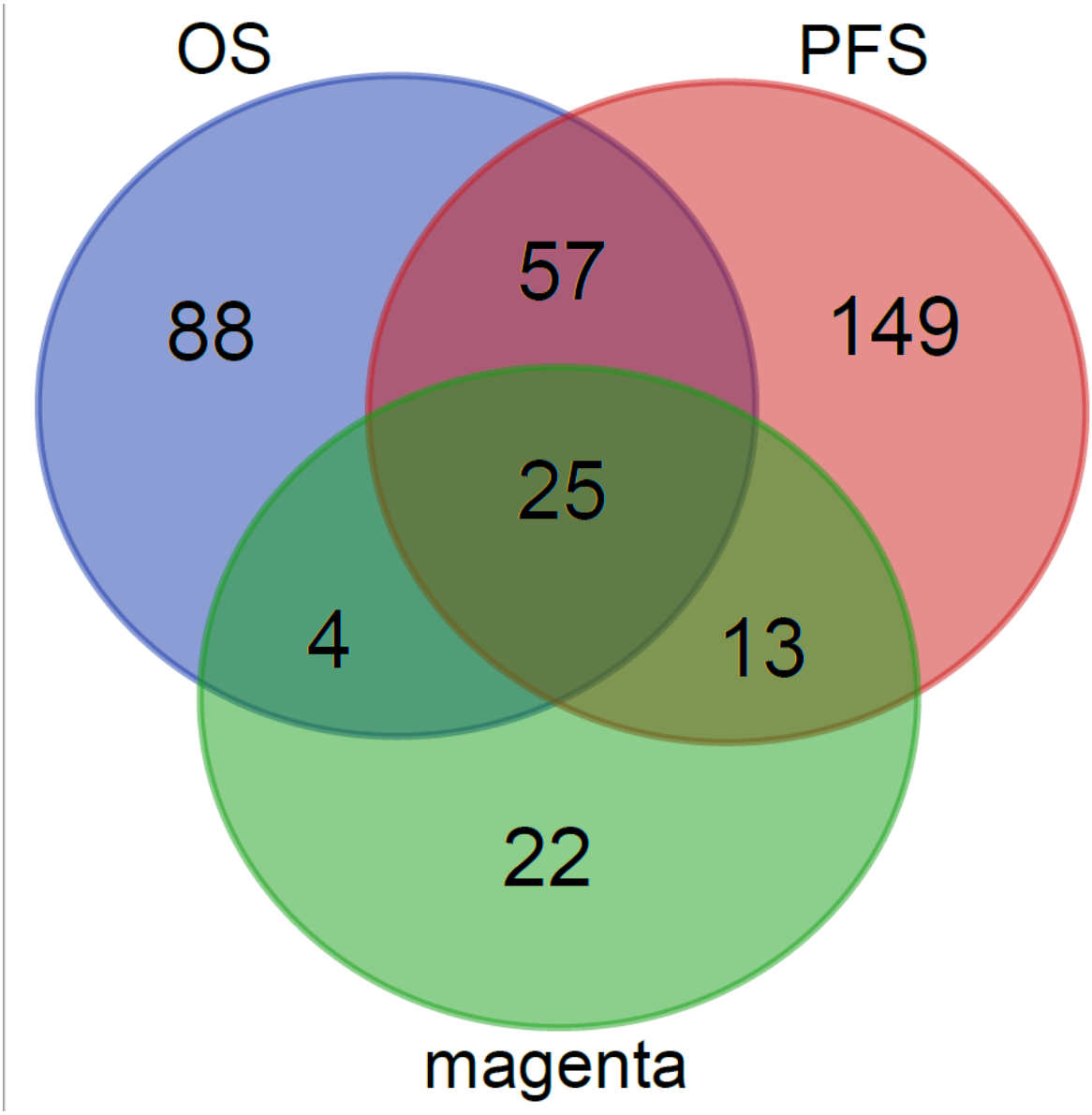

Figure 3. Identification of lncRNAs signature by overlap of OS related lncRNAs, PFS related lncRNAs and lncRNAs in magenta.

3.4. Identification of consensus clusters

The magenta module was considered as the prognostic module. The magenta module could therefore serve as candidate of prediction of survival benefit in advanced melanoma patients treated with anti-PD1 alone or in combination with anti-CTLA-4. According to cophenetic coefficient of NMF (Figure 4A), we used 9 lncRNAs (ENSG00000258869, ENSG00000179840, ENSG00000206344, ENSG00000226777, ENSG00000205018, ENSG00000204261, ENSG00000163597, ENSG00000197536, and ENSG00000263069) to cluster the population into two consensus clusters: cluster 1 (n = 49) and cluster 2 (n = 42) (Figure 4B)). There were also differences in prognostic module expression between the two clusters (Figure 4C). Furthermore, cluster 2 exhibited significantly longer OS than cluster 1 (HR=3.29, 95%CI: 1.63-6.64, P = 0.0005, Figure 4D). Regarding PFS, cluster 1 was correlated with significantly unfavorable PFS (HR=2.77, 95%CI: 1.59-3.82, P = 0.0002, Figure 4E). The identified lncRNAs could divide advanced melanoma patients into different clusters and correlated with response and survival benefit of ICI.

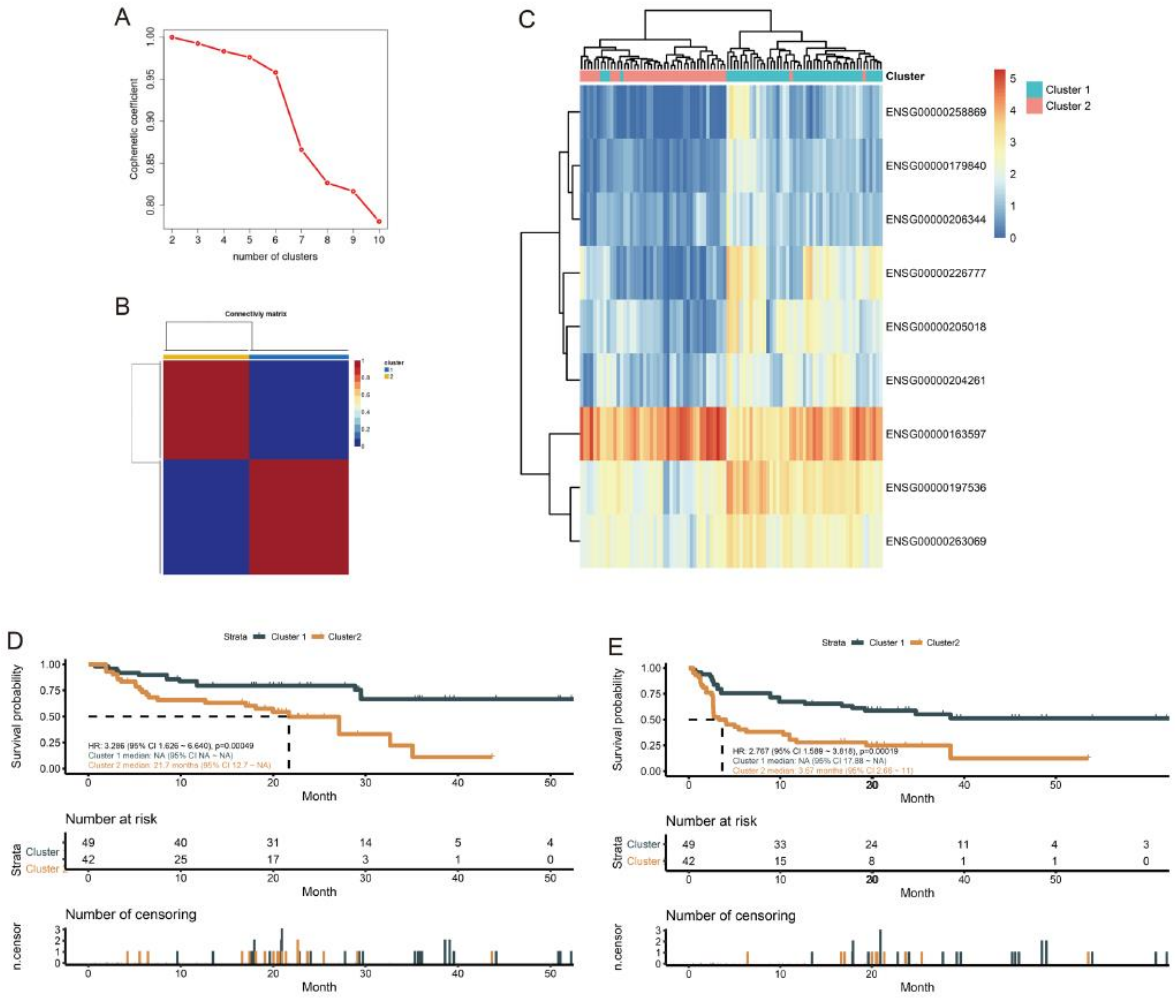

Figure 4. Identification of consensus clusters by NMF. A. The relationship between cophenetic coefficients with respect to the number of clusters. B. The consensus map of NMF clustering results. Patients were divided into cluster 1 and cluster 2 according to the prognostic module. C. The heatmap plot of prognostic module. D. The survival curve of OS in cluster 1 and cluster 2. E. The survival curve of PFS in cluster 1 and cluster 2.

3.5. Subgroup analysis

After eliminating the duplicate patients, 59 patients were left for subgroup analysis. Our identified nine lncRNAs signature could also separate population who benefit from survival (Cluster 2) regardless of OS (HR=3.41, 95%CI: 1.38-8.45, P = 0.0051, Figure 5A) and PFS (HR=2.71, 95%CI: 1.32-5.57, P = 0.0052, Figure 5B). In 25 patients receiving anti-PD-1 monotherapy, cluster 2 exhibited significantly longer OS (HR=3.11, 95%CI: 1.04-9.24, P = 0.033, Figure 5C) and PFS (HR=4.39, 95%CI: 1.41-13.64, P = 0.0057, Figure 5D) than cluster 1. Besides, cluster 2 also was correlated with significantly favorable OS (HR=7.02, 95%CI: 0.89-55.63, P = 0.032, Figure 5E) and PFS (HR=2.89, 95%CI: 0.94-8.91, P = 0.056, Figure 5F) in 34 patients treated with combined anti-PD-1 and anti-CTLA-4. The nine lncRNAs could divide advanced melanoma patients into different clusters and correlated with survival benefit from ICI, regardless of anti-PD-1 in combination with CTLA-4 or as single agent.

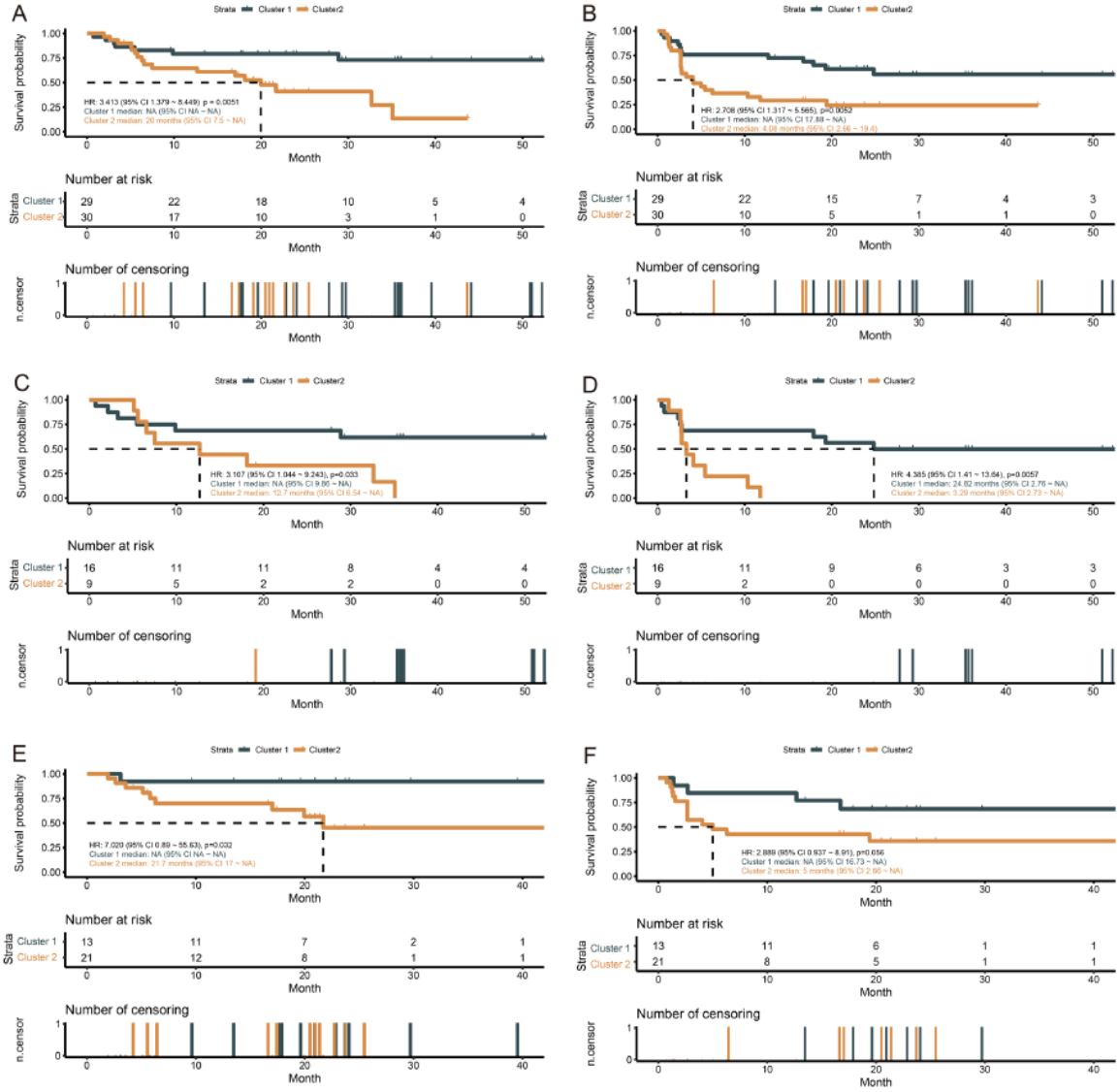

Figure 5. Subgroup analysis of consensus clusters predict survival benefit of patients treated with ICI by combined or single therapy. A. The survival curve of OS in cluster 1 and cluster 2 after de-duplication. B. The survival curve of PFS in cluster 1 and cluster 2 after de-duplication. C. The survival curve of OS of monotherapy in cluster 1 and cluster 2 after de-duplication. D. The survival curve of PFS of monotherapy in cluster 1 and cluster 2 after de-duplication. E. The survival curve of OS of combined therapy in cluster 1 and cluster 2 after de-duplication. F. The survival curve of PFS of combined therapy in cluster 1 and cluster 2 after de-duplication.

3.6. Functional analysis

We identified 2223 differentially expressed genes (DEGs) by cluster 1 vs cluster 2, including 812 up-regulated and 1411 down-regulated DEGs (Figure 6). Further enrichment analysis showed that these 2223 DEGs were enriched to 759 Gene Ontology terms: 69 molecular function defined as the biochemical activity including specific binding to ligands or structures of a gene product, 623 biological processes refereed to a biological objective to which the gene or gene product contributes, 67 cell component refereed to the place in the cell where a gene product is active) [35], and 63 Kyoto Encyclopedia of Genes and Genomes pathways, a knowledge base for systematic analysis of gene functions, linking genomic information with higher order functional information [36], respectively (Table S2) . The enrichment analysis revealed that the most enriched molecular function of DEGs were major histocompatibility complex (MHC) protein binding, MHC protein complex binding, and

immunoglobulin binding (Figure 7A, Table S2). The most enriched biological process of DEGs were immune-related cells activation and differentiation (Figure 7B, Table S2). The most enriched cell component of DEGs were MHC protein complex, MHC class II protein complex, and immunological features (Figure 7C, Table S2). The most enriched pathways of DEGs were leukocyte trans endothelial migration, T cell receptor signaling pathway, Th1 and Th2 cell differentiation, Th17 cell differentiation, B cell receptor signaling pathway, PD-L1 expression and PD-1 checkpoint pathway in cancer, natural killer cell-mediated cytotoxicity, and primary immunodeficiency (Figure 7D, Table S2).

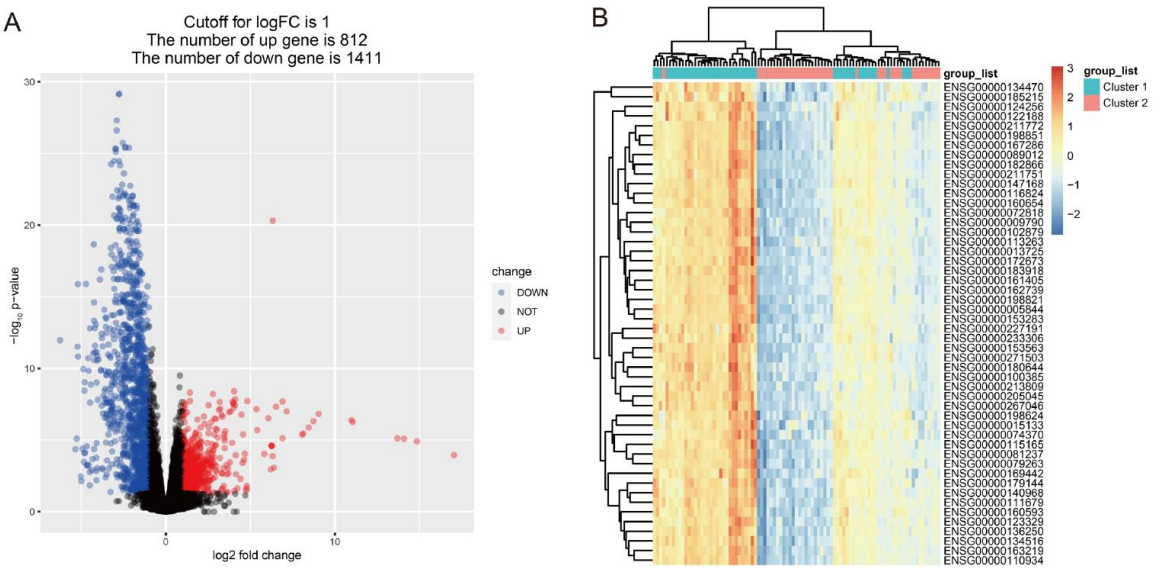

Figure 6. Identification of DEGs by cluster 1 vs cluster 2. A. The volcano plot of DEGs by cluster 1 vs cluster 2. B. The heatmap plot of DEGs by cluster 1 vs cluster 2.

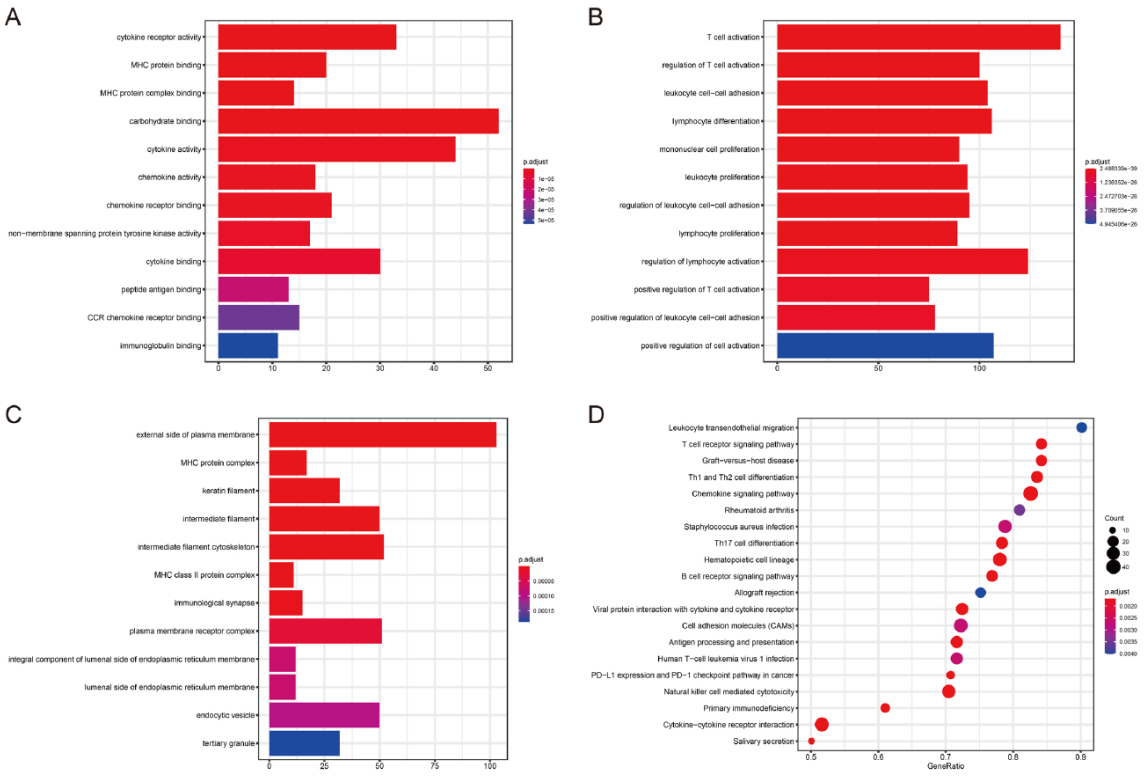

Figure 7. Functional enrichment of DEGs by cluster 1 vs cluster 2. A. The molecular function of DEGs by cluster 1 vs cluster 2. B. The biological process of DEGs by cluster 1 vs cluster 2. C. The cell component of DEGs by cluster 1 vs cluster 2. B. The pathway analysis of DEGs by cluster 1 vs cluster 2.

4. Discussion

Over the past decades, with a deeper understanding of the pathophysiology and the the manifold roles of the immune system in cancer management [37], ICI have made their way into clinics as single treatment or in multimodal settings for several tumor entities [38-40]. While these advances in the treatment of metastatic melanoma have improved responses and survival[41], still the majority of patients do not respond properly or respond with side effects to ICI. Although the regimens of ICI-based immunotherapy have been continuously adjusted and optimized [42-44], patients with melanoma still have heterogeneous ICI response. Different individuals respond differently to ICI, which requires screening for the most sensitive subgroup. An early assessment for ICI response by predictive signature is crucial for the selection of patients who are most likely to benefit from ICI. Correlation networks are more and more widely used in this field. WGCNA is a systematic biology approach to describe the correlation patterns among elements across microarray samples to find modules of highly correlated elements, which can be used to identify candidate biomarkers or therapeutic targets [26], and NMF can identify potential characteristics in expression profiles by resolving the original matrix into different nonnegative matrices [45,46]. In addition, lncRNAs are widely involved in the pathophysiological process of various tumors [47]. Hence, in this study, we combined NMF and WGCNA to discover nine prognostic lncRNAs signature for patients with melanoma, which can also reflect the ICI response, and then initially explored the potential mechanisms.

A growing body of lncRNAs has been detected and identified in various immune cells [48,49], and lncRNAs play a vital role in cancer immunology [50]. Together, these findings demonstrate the potential of lncRNAs in cancer prognosis and ICI response evaluation. In our study, a total of 9 lncRNAs (ENSG00000258869, ENSG00000179840, ENSG00000206344, ENSG00000226777, ENSG00000205018, ENSG00000204261, ENSG00000163597, ENSG00000197536, and ENSG00000263069) signature were identified by computational approach, and they can easily divide melanoma patients into two groups with different survival benefit. Furthermore, these lncRNAs signature can also reflect the response to ICI, since all of the participants that we included in this study were patients receiving anti-PD-1 monotherapy or combined anti-PD-1 and anti-CTLA-4. Subgroup analysis also showed the universality of the nine lncRNAs signature. We used the DEGs between two consensus clusters as a starting point to explore why there was such a large difference in survival benefit between the two clusters distinguished by nine lncRNAs signature.

Enrichment analysis showed that the functions of DEGs were mainly related to MHC and immune processes. The initiation of an adaptive immune response requires recognition of antigens in the context of MHC class I and class II proteins by $CD8^+$ and $CD4^+$ T cells, respectively [51-53]. Moreover, the identified pathways were also enriched for PD-L1/PD-1 axis events, which is exactly the target of ICI. Therefore, one can hypothesise that the identified nine lncRNAs signature might affect the survival benefit of advanced melanoma patients treated with ICI through MHC- and generally immune-related pathways.

However, one has to consider that our analyses are based on the publicly available dataset. Thus we could not obtain all the clinic-pathological characteristics for each patient. Furthermore, we included 91 tumor biopsies from 75 patients, indicating 16 patients provided two biopsies. A sample from a single patient may need attention in subsequent larger studies. Moreover, since the population we included in this retrospective study was melanoma patients receiving ICI with complete follow-up data, our sample size was small. Therefore, further testing and verifying of the 9 lncRNAs signature in prospective studies will be necessary.

5. Conclusions

However, we succeeded to characterize lncRNA expression profiles to identify an OS and PFS advantage of cluster 2 over cluster 1, distinguished by 9 lncRNAs signature. Further analyses provide hints that this signature affects the response of melanoma patients treated with ICI by influencing MHC- and immune-related pathways. The nine lncRNAs signature is therefore a novel predictor for OS and PFS in melanoma patients treated with ICI.

Supplementary Materials: The following are available online at www.mdpi.com/xxx/s1, Figure S1: The median rank and $Z_{summary}$ statistics of each module preservation, Table S1: Details of lncRNAs related to OS and PFS and in the magenta module, Table S2: Details of the DEGs function and pathway annotation analysis.

Author Contributions: Conceptualization: JGZ, BL, JGL, HM, USG, SHJ; methodology: JGZ, BL, JGL, BF; validation: NG, RF, MH, HM, UG, JGZ data curation: JGZ, BL, JGL, HM, USG; writing—original draft preparation: JGZ, BL; ; writing—review and editing: USG, HM, BF, JGL; visualization: JGZ, BF; supervision: HM, USG; JGZ; project administration: HM, USG; funding acquisition: HM, JGZ, SHJ;Y.Y. All authors have read and agreed to the published version of the manuscript.

Funding: This research was funded by the National Natural Science Foundation of China (Grant No. 81660512), Research Programs of Science and Technology Commission Foundation of Zunyi City (Grant Nos. HZ2019-11, HZ2019-07), Research Programs of Health Commission Foundation of Guizhou Province (Grant Nos. gzwjkj2019-1-073, gzwjkj2019-1-172).

Acknowledgments: We would like to thank Tuba N. Gide *et al*. who released and shared their data on the EMBL-EBI database. The present work was performed by Jian-Guo Zhou in (partial) fulfilment of the requirements for containing the degree "Dr. rer. biol. hum".

Conflicts of Interest: The authors declare no conflict of interest.

References

1. Nakamura, Y.; Fujisawa, Y. Diagnosis and Management of Acral Lentiginous Melanoma. *Current treatment options in oncology* **2018**, *19*, 42, doi:10.1007/s11864-018-0560-y.
2. Keung, E.Z.; Gershenwald, J.E. Clinicopathological Features, Staging, and Current Approaches to Treatment in High-Risk Resectable Melanoma. *J Natl Cancer Inst* **2020**, 10.1093/jnci/djaa012, doi:10.1093/jnci/djaa012.
3. Berk-Krauss, J.; Stein, J.A.; Weber, J.; Polsky, D.; Geller, A.C. New Systematic Therapies and Trends in Cutaneous Melanoma Deaths Among US Whites, 1986-2016. *Am J Public Health* **2020**, 10.2105/AJPH.2020.305567, e1-e3, doi:10.2105/AJPH.2020.305567.
4. Ribero, S.; Glass, D.; Bataille, V. Genetic epidemiology of melanoma. *Eur J Dermatol* **2016**, *26*, 335-339, doi:10.1684/ejd.2016.2787.
5. Hegde, P.S.; Chen, D.S. Top 10 Challenges in Cancer Immunotherapy. *Immunity* **2020**, *52*, 17-35, doi:10.1016/j.immuni.2019.12.011.
6. Eggermont, A.M.; Chiarion-Sileni, V.; Grob, J.J.; Dummer, R.; Wolchok, J.D.; Schmidt, H.; Hamid, O.; Robert, C.; Ascierto, P.A.; Richards, J.M., et al. Prolonged Survival in Stage III Melanoma with Ipilimumab Adjuvant Therapy. *The New England journal of medicine* **2016**, *375*, 1845-1855, doi:10.1056/NEJMoa1611299.
7. Weber, J.; Mandala, M.; Del Vecchio, M.; Gogas, H.J.; Arance, A.M.; Cowey, C.L.; Dalle, S.; Schenker, M.; Chiarion-Sileni, V.; Marquez-Rodas, I., et al. Adjuvant Nivolumab versus Ipilimumab in Resected Stage III or IV Melanoma. *The New England journal of medicine* **2017**, *377*, 1824-1835, doi:10.1056/NEJMoa1709030.
8. Eggermont, A.M.M.; Blank, C.U.; Mandala, M.; Long, G.V.; Atkinson, V.; Dalle, S.; Haydon, A.; Lichinitser, M.; Khattak, A.; Carlino, M.S., et al. Adjuvant Pembrolizumab versus Placebo in Resected

Stage III Melanoma. *The New England journal of medicine* **2018**, *378*, 1789-1801, doi:10.1056/NEJMoa1802357.

9. Schachter, J.; Ribas, A.; Long, G.V.; Arance, A.; Grob, J.-J.; Mortier, L.; Daud, A.; Carlino, M.S.; McNeil, C.; Lotem, M., et al. Pembrolizumab versus ipilimumab for advanced melanoma: final overall survival results of a multicentre, randomised, open-label phase 3 study (KEYNOTE-006). *Lancet* **2017**, *390*, 1853-1862, doi:10.1016/S0140-6736(17)31601-X.
10. Robert, C.; Ribas, A.; Schachter, J.; Arance, A.; Grob, J.-J.; Mortier, L.; Daud, A.; Carlino, M.S.; McNeil, C.M.; Lotem, M., et al. Pembrolizumab versus ipilimumab in advanced melanoma (KEYNOTE-006): post-hoc 5-year results from an open-label, multicentre, randomised, controlled, phase 3 study. *Lancet Oncol* **2019**, *20*, 1239-1251, doi:10.1016/S1470-2045(19)30388-2.
11. Wolchok, J.D.; Chiarion-Sileni, V.; Gonzalez, R.; Rutkowski, P.; Grob, J.-J.; Cowey, C.L.; Lao, C.D.; Wagstaff, J.; Schadendorf, D.; Ferrucci, P.F., et al. Overall Survival with Combined Nivolumab and Ipilimumab in Advanced Melanoma. *The New England journal of medicine* **2017**, *377*, 1345-1356, doi:10.1056/NEJMoa1709684.
12. Hodi, F.S.; Chiarion-Sileni, V.; Gonzalez, R.; Grob, J.-J.; Rutkowski, P.; Cowey, C.L.; Lao, C.D.; Schadendorf, D.; Wagstaff, J.; Dummer, R., et al. Nivolumab plus ipilimumab or nivolumab alone versus ipilimumab alone in advanced melanoma (CheckMate 067): 4-year outcomes of a multicentre, randomised, phase 3 trial. *Lancet Oncol* **2018**, *19*, 1480-1492, doi:10.1016/S1470-2045(18)30700-9.
13. Larkin, J.; Chiarion-Sileni, V.; Gonzalez, R.; Grob, J.-J.; Rutkowski, P.; Lao, C.D.; Cowey, C.L.; Schadendorf, D.; Wagstaff, J.; Dummer, R., et al. Five-Year Survival with Combined Nivolumab and Ipilimumab in Advanced Melanoma. *The New England journal of medicine* **2019**, *381*, 1535-1546, doi:10.1056/NEJMoa1910836.
14. Hodi, F.S.; Chesney, J.; Pavlick, A.C.; Robert, C.; Grossmann, K.F.; McDermott, D.F.; Linette, G.P.; Meyer, N.; Giguere, J.K.; Agarwala, S.S., et al. Combined nivolumab and ipilimumab versus ipilimumab alone in patients with advanced melanoma: 2-year overall survival outcomes in a multicentre, randomised, controlled, phase 2 trial. *Lancet Oncol* **2016**, *17*, 1558-1568, doi:10.1016/S1470-2045(16)30366-7.
15. Regan, M.M.; Werner, L.; Rao, S.; Gupte-Singh, K.; Hodi, F.S.; Kirkwood, J.M.; Kluger, H.M.; Larkin, J.; Postow, M.A.; Ritchings, C., et al. Treatment-Free Survival: A Novel Outcome Measure of the Effects of Immune Checkpoint Inhibition-A Pooled Analysis of Patients With Advanced Melanoma. *J Clin Oncol* **2019**, *37*, 3350-3358, doi:10.1200/JCO.19.00345.
16. Tawbi, H.A.; Forsyth, P.A.; Algazi, A.; Hamid, O.; Hodi, F.S.; Moschos, S.J.; Khushalani, N.I.; Lewis, K.; Lao, C.D.; Postow, M.A., et al. Combined Nivolumab and Ipilimumab in Melanoma Metastatic to the Brain. *The New England journal of medicine* **2018**, *379*, 722-730, doi:10.1056/NEJMoa1805453.
17. Sarropoulos, I.; Marin, R.; Cardoso-Moreira, M.; Kaessmann, H. Developmental dynamics of lncRNAs across mammalian organs and species. *Nature* **2019**, *571*, 510-514, doi:10.1038/s41586-019-1341-x.
18. Quagliata, L.; Matter, M.S.; Piscuoglio, S.; Arabi, L.; Ruiz, C.; Procino, A.; Kovac, M.; Moretti, F.; Makowska, Z.; Boldanova, T., et al. Long noncoding RNA HOTTIP/HOXA13 expression is associated with disease progression and predicts outcome in hepatocellular carcinoma patients. *Hepatology (Baltimore, Md.)* **2014**, *59*, 911-923, doi:10.1002/hep.26740.
19. Li, J.; Wang, W.; Xia, P.; Wan, L.; Zhang, L.; Yu, L.; Wang, L.; Chen, X.; Xiao, Y.; Xu, C. Identification of a five-lncRNA signature for predicting the risk of tumor recurrence in patients with breast cancer. *Int J Cancer* **2018**, *143*, 2150-2160, doi:10.1002/ijc.31573.

20. Gide, T.N.; Quek, C.; Menzies, A.M.; Tasker, A.T.; Shang, P.; Holst, J.; Madore, J.; Lim, S.Y.; Velickovic, R.; Wongchenko, M., et al. Distinct Immune Cell Populations Define Response to Anti-PD-1 Monotherapy and Anti-PD-1/Anti-CTLA-4 Combined Therapy. *Cancer Cell* **2019**, *35*, 238-255, doi:10.1016/j.ccell.2019.01.003.
21. Madeira, F.; Park, Y.M.; Lee, J.; Buso, N.; Gur, T.; Madhusoodanan, N.; Basutkar, P.; Tivey, A.R.N.; Potter, S.C.; Finn, R.D., et al. The EMBL-EBI search and sequence analysis tools APIs in 2019. *Nucleic Acids Res* **2019**, *47*, W636-W641, doi:10.1093/nar/gkz268.
22. Dobin, A.; Davis, C.A.; Schlesinger, F.; Drenkow, J.; Zaleski, C.; Jha, S.; Batut, P.; Chaisson, M.; Gingeras, T.R. STAR: ultrafast universal RNA-seq aligner. *Bioinformatics* **2013**, *29*, 15-21, doi:10.1093/bioinformatics/bts635.
23. Li, B.; Dewey, C.N. RSEM: accurate transcript quantification from RNA-Seq data with or without a reference genome. *BMC Bioinformatics* **2011**, *12*, 323, doi:10.1186/1471-2105-12-323.
24. Jin, S.-H.; Zhou, R.-H.; Guan, X.-Y.; Zhou, J.-G.; Liu, J.-G. Identification of novel key lncRNAs involved in periodontitis by weighted gene co-expression network analysis. *J. Periodontal Res.* **2020**, *55*, 96-106, doi:10.1111/jre.12693.
25. Zhang, B.; Horvath, S. A general framework for weighted gene co-expression network analysis. *Stat Appl Genet Mol Biol* **2005**, *4*, Article17.
26. Langfelder, P.; Horvath, S. WGCNA: an R package for weighted correlation network analysis. *BMC Bioinformatics* **2008**, *9*, 559, doi:10.1186/1471-2105-9-559.
27. Langfelder, P.; Zhang, B.; Horvath, S. Defining clusters from a hierarchical cluster tree: the Dynamic Tree Cut package for R. *Bioinformatics* **2008**, *24*, 719-720.
28. Langfelder, P.; Horvath, S. Eigengene networks for studying the relationships between co-expression modules. *BMC Syst Biol* **2007**, *1*, 54.
29. Kushwaha, G.; Dozmorov, M.; Wren, J.D.; Qiu, J.; Shi, H.; Xu, D. Hypomethylation coordinates antagonistically with hypermethylation in cancer development: a case study of leukemia. *Hum Genomics* **2016**, *10 Suppl 2*, 18, doi:10.1186/s40246-016-0071-5.
30. Horvath, S.; Zhang, Y.; Langfelder, P.; Kahn, R.S.; Boks, M.P.M.; van Eijk, K.; van den Berg, L.H.; Ophoff, R.A. Aging effects on DNA methylation modules in human brain and blood tissue. *Genome Biol* **2012**, *13*, R97, doi:10.1186/gb-2012-13-10-r97.
31. Zhou, J.-G.; Liang, B.; Jin, S.-H.; Liao, H.-L.; Du, G.-B.; Cheng, L.; Ma, H.; Gaipl, U.S. Development and Validation of an RNA-Seq-Based Prognostic Signature in Neuroblastoma. *Frontiers in Oncology* **2019**, *9*, 1361, doi:10.3389/fonc.2019.01361.
32. Gaujoux, R.; Seoighe, C. A flexible R package for nonnegative matrix factorization. *BMC Bioinformatics* **2010**, *11*, 367, doi:10.1186/1471-2105-11-367.
33. Robinson, M.D.; McCarthy, D.J.; Smyth, G.K. edgeR: a Bioconductor package for differential expression analysis of digital gene expression data. *Bioinformatics* **2010**, *26*, 139-140, doi:10.1093/bioinformatics/btp616.
34. Yu, G.-C.; Wang, L.-G.; Han, Y.-Y.; He, Q.-Y. clusterProfiler: an R package for comparing biological themes among gene clusters. *OMICS* **2012**, *16*, 284-287, doi:10.1089/omi.2011.0118.
35. Ashburner, M., .; Ball, C.A.; Blake, J.A.; Botstein, D., .; Butler, H., .; Cherry, J.M.; Davis, A.P.; Dolinski, K., .; Dwight, S.S.; Eppig, J.T. Gene ontology: tool for the unification of biology. The Gene Ontology Consortium. *Nat. Genet.* **2000**, *25*, 25-28.

36. Kanehisa, M.; Goto, S. KEGG: Kyoto Encyclopaedia of Genes and Genomes. *Nucleic Acids Res.* **2000**, *28*, 27-30.
37. Rückert, M.; Deloch, L.; Fietkau, R.; Frey, B.; Hecht, M.; Gaipl, U.S. Immune modulatory effects of radiotherapy as basis for well-reasoned radioimmunotherapies. *Strahlentherapie und Onkologie : Organ der Deutschen Rontgengesellschaft ... [et al]* **2018**, *194*, 509-519, doi:10.1007/s00066-018-1287-1.
38. Franklin, C.; Livingstone, E.; Roesch, A.; Schilling, B.; Schadendorf, D. Immunotherapy in melanoma: Recent advances and future directions. *European journal of surgical oncology : the journal of the European Society of Surgical Oncology and the British Association of Surgical Oncology* **2017**, *43*, 604-611, doi:10.1016/j.ejso.2016.07.145.
39. Havel, J.J.; Chowell, D.; Chan, T.A. The evolving landscape of biomarkers for checkpoint inhibitor immunotherapy. *Nat Rev Cancer* **2019**, *19*, 133-150, doi:10.1038/s41568-019-0116-x.
40. Kokowski, K.; Stangl, S.; Seier, S.; Hildebrandt, M.; Vaupel, P.; Multhoff, G. Radiochemotherapy combined with NK cell transfer followed by second-line PD-1 inhibition in a patient with NSCLC stage IIIb inducing long-term tumor control: a case study. *Strahlentherapie und Onkologie : Organ der Deutschen Rontgengesellschaft ... [et al]* **2019**, *195*, 352-361, doi:10.1007/s00066-019-01434-9.
41. Amaria, R.N.; Menzies, A.M.; Burton, E.M.; Scolyer, R.A.; Tetzlaff, M.T.; Antdbacka, R.; Ariyan, C.; Bassett, R.; Carter, B.; Daud, A., et al. Neoadjuvant systemic therapy in melanoma: recommendations of the International Neoadjuvant Melanoma Consortium. *Lancet Oncol* **2019**, *20*, e378-e389, doi:10.1016/S1470-2045(19)30332-8.
42. Weber, J.; Glutsch, V.; Geissinger, E.; Haug, L.; Lock, J.F.; Schneider, F.; Kneitz, H.; Goebeler, M.; Schilling, B.; Gesierich, A. Neoadjuvant immunotherapy with combined ipilimumab and nivolumab in patients with melanoma with primary or in transit disease. *Br J Dermatol* **2019**, 10.1111/bjd.18739, doi:10.1111/bjd.18739.
43. Pelster, M.S.; Amaria, R.N. Neoadjuvant Immunotherapy for Locally Advanced Melanoma. *Current treatment options in oncology* **2020**, *21*, 10, doi:10.1007/s11864-020-0700-z.
44. Lebbé, C.; Meyer, N.; Mortier, L.; Marquez-Rodas, I.; Robert, C.; Rutkowski, P.; Menzies, A.M.; Eigentler, T.; Ascierto, P.A.; Smylie, M., et al. Evaluation of Two Dosing Regimens for Nivolumab in Combination with Ipilimumab in Patients With Advanced Melanoma: Results From the Phase IIIb/IV CheckMate 511 Trial. *Journal of clinical oncology* **2019**, *37*, 867-875, doi:10.1200/JCO.18.01998.
45. Brunet, J.-P.; Tamayo, P.; Golub, T.R.; Mesirov, J.P. Metagenes and molecular pattern discovery using matrix factorization. *Proc Natl Acad Sci USA* **2004**, *101*, 4164-4169.
46. Jiao, C.-N.; Gao, Y.-L.; Yu, N.; Liu, J.-X.; Qi, L.-Y. Hyper-graph Regularized Constrained NMF for Selecting Differentially Expressed Genes and Tumor Classification. *IEEE J Biomed Health Inform* **2020**, 10.1109/JBHI.2020.2975199, doi:10.1109/JBHI.2020.2975199.
47. Luo, X.; Qiu, Y.; Jiang, Y.; Chen, F.; Jiang, L.; Zhou, Y.; Dan, H.; Zeng, X.; Lei, Y.L.; Chen, Q. Long non-coding RNA implicated in the invasion and metastasis of head and neck cancer: possible function and mechanisms. *Mol Cancer* **2018**, *17*, 14, doi:10.1186/s12943-018-0763-7.
48. Chen, Y.G.; Satpathy, A.T.; Chang, H.Y. Gene regulation in the immune system by long noncoding RNAs. *Nature immunology* **2017**, *18*, 962-972, doi:10.1038/ni.3771.
49. Elling, R.; Chan, J.; Fitzgerald, K.A. Emerging role of long noncoding RNAs as regulators of innate immune cell development and inflammatory gene expression. *European journal of immunology* **2016**, *46*, 504-512, doi:10.1002/eji.201444558.

50. Yu, Y.; Zhang, W.; Li, A.; Chen, Y.; Ou, Q.; He, Z.; Zhang, Y.; Liu, R.; Yao, H.; Song, E. Association of Long Noncoding RNA Biomarkers With Clinical Immune Subtype and Prediction of Immunotherapy Response in Patients With Cancer. *JAMA Netw Open* **2020**, *3*, e202149, doi:10.1001/jamanetworkopen.2020.2149.

51. Łuksza, M.; Riaz, N.; Makarov, V.; Balachandran, V.P.; Hellmann, M.D.; Solovyov, A.; Rizvi, N.A.; Merghoub, T.; Levine, A.J.; Chan, T.A., et al. A neoantigen fitness model predicts tumour response to checkpoint blockade immunotherapy. *Nature* **2017**, *551*, 517-520, doi:10.1038/nature24473.

52. Cañadas, I.; Thummalapalli, R.; Kim, J.W.; Kitajima, S.; Jenkins, R.W.; Christensen, C.L.; Campisi, M.; Kuang, Y.; Zhang, Y.; Gjini, E., et al. Tumor innate immunity primed by specific interferon-stimulated endogenous retroviruses. *Nat Med* **2018**, *24*, 1143-1150, doi:10.1038/s41591-018-0116-5.

53. Rodig, S.J.; Gusenleitner, D.; Jackson, D.G.; Gjini, E.; Giobbie-Hurder, A.; Jin, C.; Chang, H.; Lovitch, S.B.; Horak, C.; Weber, J.S., et al. MHC proteins confer differential sensitivity to CTLA-4 and PD-1 blockade in untreated metastatic melanoma. *Science translational medicine* **2018**, *10*, doi:10.1126/scitranslmed.aar3342.

Table and figures legend

Table 1. Patient characteristics of PRJEB23709 dataset.

Figure 1. Sample clustering dendrogram and determination of soft-thresholding power in WGCNA. A. Sample clustering dendrogram to detect outliers. B. Analysis of the scale-free fit index for various soft-thresholding power. C. Analysis of the mean connectivity for various soft-thresholding powers.

Figure 2. Identify key module related OS and PFS by WGCNA. A. Clustering dendrogram of lncRNAs with dissimilarity based on topological overlap together and assigned module colors. B. The heatmap plot of visualizing all modules. C. The module- trait heatmap plot.

Figure 3. Identification of lncRNAs signature by overlap of OS related lncRNAs, PFS related lncRNAs and lncRNAs in mageta.

Figure 4. Identification of consensus clusters by NMF. A. The relationship between cophenetic coefficients with respect to the number of clusters. B. The consensus map of NMF clustering results. Patients were divided into cluster 1 and cluster 2 according to the prognostic module. C. The heatmap plot of prognostic module. D. The survival curve of OS in cluster 1 and cluster 2. E. The survival curve of PFS in cluster 1 and cluster 2.

Figure 5. Subgroup analysis of consensus clusters predict survival benefit of patients treated with ICI by combined therapy or alone. A. The survival curve of OS in cluster 1 and cluster 2 after de duplication. B. The survival curve of PFS in cluster 1 and cluster 2 after de duplication. C. The survival curve of OS of monotherapy in cluster 1 and cluster 2 after de duplication. D. The survival curve of PFS of monotherapy in cluster 1 and cluster 2 after de duplication. E. The survival curve of OS of combined therapy in cluster 1 and cluster 2 after de duplication. F. The survival curve of PFS of combined therapy in cluster 1 and cluster 2 after de duplication.

Figure 6. Identification of DEGs by cluster 1 vs cluster 2. A. The volcano plot of DEGs by cluster 1 vs cluster 2. B. The heatmap plot of DEGs by cluster 1 vs cluster 2.

Figure 7. Functional enrichment of DEGs by cluster 1 vs cluster 2. A. The molecular function of DEGs by cluster 1 vs cluster 2. B. The biological process of DEGs by cluster 1 vs cluster 2. C. The cell component of DEGs by cluster 1 vs cluster 2. B. The pathway analysis of DEGs by cluster 1 vs cluster 2.